Reciprocal metabolism of ^{18}F-PSMA-1007 and ^{18}F-FDG PET/CT in patients with prostate cancer at staging

Jisu Kim

Department of Medicine

The Graduate School, Yonsei University

Reciprocal metabolism of ^{18}F-PSMA-1007 and ^{18}F-FDG PET/CT in patients with prostate cancer at staging

Jisu Kim

Department of Medicine

The Graduate School, Yonsei University

Reciprocal metabolism of ^{18}F-PSMA-1007 and ^{18}F-FDG PET/CT in patients with prostate cancer at staging

Directed by Professor Mijin Yun

The Master's Thesis
submitted to the Department of Medicine,
the Graduate School of Yonsei University
in partial fulfillment of the requirements for the degree of
Master of Medical Science

Jisu Kim

December 2022

This certifies that the Master's Thesis of
Jisu Kim is approved.

[Signature]

Thesis Supervisor : Mijin Yun

[Signature]

Thesis Committee Member#1 : Young Deuk Choi

[Signature]

Thesis Committee Member#2 : Misu Lee

The Graduate School
Yonsei University

December 2022

ACKNOWLEDGEMENTS

There are many people who have helped me a lot in the process of writing this dissertation. I am writing this to express my gratitude to them.

I would like to express my gratitude to my advisor, Prof. Mijin Yun, who allowed me to conduct research on the thesis topic above and spared no effort in guiding me. And I would like to express my gratitude to Prof. Misu Lee of Incheon National University, who provided great help and advice and encouragement in the progress of the thesis. In addition, I would like to express special thanks to Prof. Young Deuk Choi for his substantial help in the evaluation and the thesis.

I couldn't mention it on paper, but there were many people who gave me a lot of mental support and help, so I would like to express my sincere gratitude to them. In the future, I will work even harder to improve myself as a researcher.

<TABLE OF CONTENTS>

LIST OF FIGURES

LIST OF TABLES

ABSTRACT

Reciprocal metabolism of ^{18}F-PSMA-1007 and ^{18}F-FDG PET/CT in patients with prostate cancer at staging

Jisu Kim

Department of Medicine
The Graduate School, Yonsei University

(Directed by Professor Mijin Yun)

Prostate cancer is a malignant tumor of the prostate and is known worldwide as the second most common cancer among men who die of cancer. PSA blood tests are usually performed in the early stages, and the higher the PSA level, the more likely it is prostate cancer. However, only about 25% of men with high PSA levels are actually diagnosed with prostate cancer through a biopsy. Therefore, there is a need for a more stable and accurate prostate cancer diagnosis and detection method in the early stages of prostate cancer diagnosis.

PSMA is an enzyme specific for prostate cancer and encoded by the human *FOLH1* gene. It was confirmed that the expression of PSMA was increased in prostate cancer patients than in normal prostate. The expression level of PSMA in prostate cancer varies depending on the pathological condition of the prostate cancer, which is closely related to the patient's prognosis. This difference in the expression level of PSMA can be a useful imaging target for prostate cancer patients, and it is being used for diagnosis and treatment of prostate cancer through radiographic imaging.

Cancer cells cause hypoxia by abnormal blood vessel formation and growth. In hypoxia-induced cancer, the expression of several proteins can be induced or inhibited by hypoxia-inducible factor (HIF). Also, due to the Warburg effect, glucose metabolism increases as well as glucose absorption rate, which can increase the expression of glucose transport pathway proteins (GLUTs), thus enabling glucose-targeted PET/CT imaging.

Therefore, even in prostate cancer, the malignancy of cancer can be tracked through image analysis using ^{18}F-FDG uptake along with PSMA. To find a new diagnostic criterion for early prostate cancer for prostate cancer by comparing SUV_{max} between ^{18}F-PSMA-1007 and ^{18}F-FDG PET/CT images and analyzing PSMA expression in *in-vitro* and *in-vivo*.

Key words : PSMA, GLUT1, PET/CT, ^{18}F-PSMA-1007, ^{18}F-FDG, Hypoxia

Reciprocal metabolism of ^{18}F-PSMA-1007 and ^{18}F-FDG PET/CT in patients with prostate cancer at staging

Jisu Kim

Department of Medicine
The Graduate School, Yonsei University

(Directed by Professor Mijin Yun)

I. INTRODUCTION

Prostate cancer (PCa) is one of the most commonly diagnosed solid malignancy in men, and it remains the second cause of male cancer-related death worldwide [1]. The traditional diagnosis for PCa is digital rectal examination and prostate-specific antigen (PSA) blood test, followed by transrectal ultrasound- or magnetic resonance imaging (MRI)- guided biopsy. However, only approximately 25% of men with elevated PSA levels are actually diagnosed with PCa through a biopsy [2]. Hence, there is an urgent need for more reliable and accurate method to detect PCa.

Prostate specific membrane antigen (PSMA) is a unique membrane-bound glycoprotein that is expressed up to several thousand-fold higher in PCa than in benign prostatic lesions [3]. In some cancers, PSMA expression can be seen in the neovasculature, but, in PCa, it is specific to cancer cells, making it a promising imaging target for patients with PCa. ^{18}F-PSMA-1007 was developed as a novel PSMA-based radiopharmaceutical for imaging PCa alternative to ^{68}Ga-PSMA-11. Recent studies showed that detection rates of ^{18}F- PSMA-1007 were comparable to or higher than ^{68}Ga-labeled PSMA ligands in patients with biochemical failure. Moreover, hepatobiliary elimination seems to be another advantage

for ^{18}F-PSMA-1007. PCa is considered histologically heterogeneous, exhibiting a wide range of PSMA expression and ^{18}F-PSMA-1007 uptake. Imaging heterogeneity of PCa may have significant implications on the patient selection and treatment [4]. Despite the evidence accumulated to date, the heterogeneity of PSMA PET signal following the aggressiveness of cancer and Gleason score remains unclear.

Typically, cancer cell metabolism is characterized by an enhanced uptake and utilization of glucose, a phenomenon known as the Warburg effect [5]. PET/CT combined with ^{18}F-FDG, as a glucose analog, had been widely used for diagnosing, staging, detecting recurrence, and predicting response to therapies in many cancers [6]. Regardless, the detection of primary tumors with high ^{18}F-FDG uptake is of clinical importance, since PCa with positive ^{18}F-FDG uptake has been associated with aggressive behavior and castration resistance [7]. PCa is known to exhibit a wide range of PSMA expression and PSMA-targeted radiotracer uptake due to histological heterogeneity. Such tumoral heterogeneity of PSMA expression and uptake can have significant implications on the patient selection and treatment [8]. Although high PSMA radiotracer uptake is generally correlated with high Gleason score (GS), it is unknown whether low PSMA uptake is associated with clinicopathologic characteristics, such as tumor aggressiveness.

To date, only few papers are available about combined analysis of ^{18}F-FDG and ^{68}Ga/^{18}F-PSMA PET/CT in primary PCa, while the majority report a single analysis [4, 9, 10]. Recently, Shi et al. retrospectively analyzed differences in lymph node metastases (LNM) from peripheral ganglia by dual ^{68}Ga-PSMA-11 and ^{18}F-FDG PET-CT in patients with undergone radical prostatectomy or treated with postoperative prostate radiotherapy [10]. However, there are no clear data to examine tumor heterogeneity by comparing the preoperative tracer uptake of ^{18}F-PSMA-1007 and ^{18}F-FDG PET/CT in patients who underwent prostatectomy. The aim of this study was to investigate the correlation between ^{18}F-PSMA-1007 and ^{18}F-FDG uptake in PCa patients before prostatectomy and how it associated with various histological subtypes.

II. MATERIALS AND METHODS

1. Study subjects

This prospective study included 42 patients with prostate cancer who underwent both ^{18}F-PSMA-1007 and ^{18}F-FDG PET/CT at initial staging between June 2019 and January 2021. Both PET/CT scans were obtained within 1 week of each other and radical prostatectomy was performed within a median 7 days of imaging (range: 5-15). This prospective study was approved by the Institutional Review Board of the Yonsei University Health System (IRB No. 4-2018-1212), and informed consent was obtained from all patients. This study was registered in the Clinical Research Information Service (CRIS) at cris.nih.go.kr (KCT0004476).

2. PET/CT imaging protocol

For ^{18}F-PSMA-1007 scan, approximately 250 MBq of ^{18}F-PSMA-1007 was administered intravenously 90 min before image acquisition. Images from the cerebellum to the proximal thighs were acquired using a PET/CT scanner (Discovery 710; General Electric Medical Systems, Milwaukee, WI, USA) with a low-dose CT transmission scan (60 mA, 120 kVp). PET emission scans were performed for 2.5 min per bed in three-dimensional mode. All patients fasted for at least 6 h before ^{18}F-FDG PET/CT scan to make sure blood glucose levels no higher than 140 mg/dL. Approximately 5.5 MBq of ^{18}F-FDG per kilogram of body weight was administered intravenously 1 hour before image acquisition. Images from the cerebellum to the proximal thighs were acquired using a PET/CT scanner (Biograph TruePoint 40; Siemens Healthcare, Erlangen, Germany) with a low-dose CT transmission scan (auto mA, 120 kVp). PET emission scans were performed for 2.5 min per bed in three-dimensional mode. PET images were reconstructed iteratively with attenuation correction, scatter, and random corrections.

3. Image analysis

^{18}F-PSMA-1007 PET/CT images were registered on the imaging software MIM (MIM-6.5; MIM Software Inc., Cleveland, OH, USA). Then, the tumour marked slides were matched with the ^{18}F-PSMA-1007 PET/CT images. A region of interest (ROI) was drawn over the tumour which marked by pathologists to measure the standardised uptake value (SUV), and the maximum SUV (SUV_{max}) was calculated as follows: (decay-corrected activity [kBq]/tissue volume [mL])/(injected ^{18}F-FDG activity [kBq]/body mass [g]).

4. Histological evaluation

Whole-mount histological slices were cut from the prostatectomy specimens. From these, hematoxylin-eosin stained whole–mount pathology slides were obtained on which a pathologist delineated the tumours. Immunohistochemistry IHC staining was performed using the Ventana Discovery automated staining system (Ventana Medical System). In brief, slides were incubated at room temperature with primary antibody: anti-PSMA rabbit monoclonal antibody (Cell signalling technology; #12702), anti-GLUT1 mouse monoclonal antibody (abcam; ab40084) and detected with the ultraView Universal DAB Detection Kit (Ventana MedicalSystem). All slides were then marked during microscopic evaluation to outline the boundaries of all foci of invasive carcinoma. Types and Gleason score of these cancer foci were evaluated.

5. RNA-Sequencing analysis

LNCaP cells were cultured in RPMI-1640 (Thermo Fisher Scientific). Medium were supplemented with 10% FBS (Hyclone, Logan, UT, USA) and 1% penicillin/streptomycin. For RNA expression profiling, total RNAs were extracted from LNCaP cells after incubation under normoxia (21% O_2) or hypoxia (1% O_2) using RNeasy Mini Kit

(QIAGEN). RNA-Sequencing and data analysis were assessed by EBIOGEN Inc.

6. LNCaP-xenograft animal model

All animal experiments were approved by The Institutional Animal Care and Use Committee of Yonsei University Health System (approval number:2020-0242). Four-to-five–week-old male BALB/c nude mice were purchased from OrientBio. LNCaP cells (2×10^6 cells/100 μl RPMI1640) mixed with 100 μL matrigel were subcutaneously injected in the right leg of each mouse. After 5-6 weeks, we collected tumor tissues and fixed with 4% formaldehyde.

7. Western blotting and immunostaining

LNCaP cells after incubation under normoxia (21% O_2) or hypoxia (1% O_2). After protein extraction using SDS lysis buffer, WB were performed following the previous protocol [11] Immunostaining of human/animal tissues and cells was performed as previously described [12, 13]. Images were acquired using an LSM710 confocal microscope and Olympus BX53 microscope with Olympus Cell Sens software (Carl Zeiss Microscopy GmbH). Each experiment had four scans per slides and analysis was performed using ImageJ software and ZEISS Zen Blue 2.6. The primary antibodies in the present study for WB and immunostaining are listed in Table 2.

8. Statistical analysis

Statistical analyses were performed using GraphPad Prism software (GraphPad Software Inc.). Results are expressed as means ± SEM (range). Statistical significance was set at $P < 0.05$. The values between multi-groups were calculated using Kruskall Wallis test, Bonferroni Post hoc analysis, and unpaired-T test.

III. RESULTS

1. Patients' characteristics

42 patients were included in this analysis. They ranged in age from 57 to 85 with a median age of 70. In the 42 patients, we selected the largest nodule as index tumor and performed further analysis. PSA values were 3.02-265.1 ng/ml, with a median of 11 ng/ml. The lesions were categorized into either acinar or ductal type based on the largest section of the tumor in each tumor region. There were 64% (27/42) of tumor lesions were dominantly acinar and 36% (15/42) were dominantly ductal type. In acinar tumors, there were 3 tumors with GS 6, 14 with GS 7, 2 with GS 8, and 8 with GS 9 or 10. In ductal tumors, there 8 were 12 lesions with GS 8 and 3 with GS 9. Detailed characteristics of all included patients are summarized in Table 1.

2.The SUV_{max} of ^{18}F-PSMA-1007 and ^{18}F-FDG in patients with acinar and ductal dominant type according to GS

All 42 index tumor lesions in 42 patients were detected by ^{18}F-PSMA-1007. 42 index tumors were classified into two groups of histological subtype, acinar dominant type and ductal dominant type. Ductal type tumors were significantly higher SUV_{max} of ^{18}F-PSMA-1007 compared with acinar type tumors (p value < 0.05). When tumors were classified according to GS, PCa patients with higher GS (>7) had significantly higher SUV_{max} of ^{18}F-PSMA-1007 compared with lower GS (Acinar GS 6-7 vs Acinar GS 8-10, p value < 0.05, Fig 1A, 1B), suggesting that tumor aggressiveness with higher GS (>7) of patients with acinar type PCa was associated with increased value of SUV_{max} of ^{18}F-PSMA-1007. In histological type, the SUV_{max} of ^{18}F -FDG was higher in ductal compared with acinar dominant type (p value < 0.05, Fig 1C, 1D), especially according to GS there was no significance between acinar low GS and acinar high GS, but ductal type tumor was significantly higher than acinar low GS (Fig 1C).

Tumor was classified as an index tumor, and correlations such as PSMA uptake and FDG uptake were confirmed. The positive correlation between index tumor and PSMA uptake showed significance (p value < 0.05, Fig 1E), and the correlation between FDG uptake tended to show significance (p value = 0.0745, Fig 1F).

3. Immunohistochemical parameters in tumor lesion of patients with acinar and ductal dominant type

Among 42 PCa patients, index tumors from 15 patient showed portion of ^{18}F-FDG uptake in the tumor. Moreover, there was a flip-flop phenomenon between ^{18}F-PSMA-1007 and ^{18}F-FDG uptake; the foci of increased ^{18}F-FDG uptake showed low ^{18}F-PSMA-1007 uptake and vice versa (Fig 2A-2C). Most (n=11) of the tumors with ^{18}F-FDG uptake were ductal type. Moreover, they were larger in size than the rest of the d FDG positive uptake tumors (n=15) without ^{18}F-FDG uptake (p-value < 0.05, Fig 2D).

Next, metabolic patterns on PET/CT scans in the primary tumors were further correlated with IHC of relevant proteins (PSMA for PSMA uptake, GLUT1 for FDG uptake) on tumor specimen. The expression of androgen receptor (AR), a key prostate cancer drug target of PCa were also determined. Tumor regions with high ^{18}F-PSMA but low ^{18}F-FDG uptake showed high PSMA and AR expressions but low GLUT1 expression. In contrast, regions with high ^{18}F-FDG but low ^{18}F-PSMA-1007 uptake revealed high GLUT1 but low PSMA and AR expressions (Fig 2B). Altogether, glycolytic tumor lesions with high uptake of ^{18}F-FDG and expression of GLUT1 showed low uptake of ^{18}F-PSMA and the expression of PSMA and AR.

4. Downregulation of PSMA expression in prostate cancer cell upon glycolytic condition in vitro

PCa cell line (LNCaP) upon hypoxia was used to validate the PSMA expression in glycolytic condition. Similar to tumor regions in patients with ductal type, the expression of PSMA was downregulated, whereas GLUT1 was upregulated in LNCaP cells under hypoxic condition (Fig 3A). Also, LNCaP cells were incubated with various concentration of $CoCl_2$, a commonly used hypoxia-mimetic agent. The expression of GLUT1 and HIF1α was dose-dependently increased after $CoCl_2$ treatment (Fig 3B). HIF1α-overexpressed LNCaP cells were also induced in the reduction of the expression of PSMA. In addition, the expression of AR was slightly downregulated in glycolytic cells (Fig 3C). To investigate the change of gene expression in glycolytic PCa cell, gene expression profile was performed in LNCaP cells after incubation under 21% O_2 (normoxia) or 1% O_2 (hypoxia) for 24h or 48h. Total 25,737 and 2,786 genes were dysregulated after 24h and 48h hypoxic condition compared with normoxia, respectively. The dysregulated genes were mainly associated with the metabolism-related categories (Fig 3D), such as fructose and mannose metabolism, glycolysis/gluconeogenesis, and carbon metabolism. Among dysregulated genes, the expression level of *FOLH1* (fold change:0.478) and *AR* (fold change:0.478) was downregulated and *HIF1a* (fold change:2.083) and *SLC2A1* (fold change:6.077) was upregulated after 48h hypoxic condition (Fig 3E). The localization of HIF1a, GLUT1 and AR affect the biological function. Thus, co-immunocytochemistry (ICC) was performed in LNCaP cells under normoxia and hypoxic condition. LNCaP cells upon hypoxic condition induced the high expression of nuclear HIF1a and membranous GLUT1, whereas downregulation of membranous PSMA and nuclear AR expression (Fig 4A). Thus, we determined that glycolytic PCa cells induced by hypoxic condition have reduced expression of PSMA and AR at both gene and protein level.

5. Downregulation of PSMA expression in tumor regions with high glycolysis in LNCaP-bearing animal model and human patients with ductal type PCa.

To validate the PSMA expression in glycolytic PCa, an *in vivo* animal model was generated by subcutaneous injection of LNCaP cells in a mouse model. The large tumor in LNCaP-xenograft model contained glycolytic tumor region with increased expression level of hypoxic/glycolytic markers, such as GLUT, HIF1α and CA9. Consistent with in *in vitro* experiment and immunostaining of human patients with PCa, tumor regions with elevated expression of GLUT1, nuclear HIF1α and CA9 in LNCaP-bearing animal model have reduced expression of PSMA (Fig 5A-5C). Downregulated AR expression was also observed in tumor regions with lower expression of PSMA (Fig 5D). Hence, the reciprocal expression pattern of PSMA and glycolytic-related protein expression was observed in *in vitro* and *in vivo* animal model.

Table 1. Patient characteristics.

				Adenocarcinoma			
				Acinar dominant		Ductal dominant	
				N	%	*N*	%
Patients (n)		42					
Index tumors (n)		42		27	64%	15	36%
Age (years)							
Median (range)		70 (50-85)					
PSA (ng/mL)							
Median (range)		11 ng/mL (3.02-265.1)					
Gleason score (n of tumors)							
6		3		3	100%	0	0%
7a		7		7	100%	0	0%
7b		7		7	100%	0	0%
8		14		2	14%	12	86%
9-10		11		8	73%	3	27%
pStage							
II	IIB	1	2%				
	IIC	8	19%				
III	IIIB	15	36%				
	IIIC	13	31%				
IV	IVA	3	7%				
	IVB	2	5%				
Tumor size (cc)							
Median (range)		2.2 (0.2-20)					

Table 2. Antibody list

Protein	Antibody	Company	Antibody dilution	
			WB	Immunostaining
HIF1α	36169	Cell signaling	1:1000	1:100
PSMA	12702	Cell signaling	1:4000	1:500
	NB1-45057	NOVUS		1:500
GLUT1	ab115730	Abcam	1:5000	
	ab40084	Abcam		1:500
	66290-1-Ig	proteintech		1:500
Pimonidazole	HP FITC MAb-1	HPI		1:100
Androgen receptor	5153	Cell signaling	1:2000	1:500
β-actin	SC-47778	Santa cruz	1:5000	

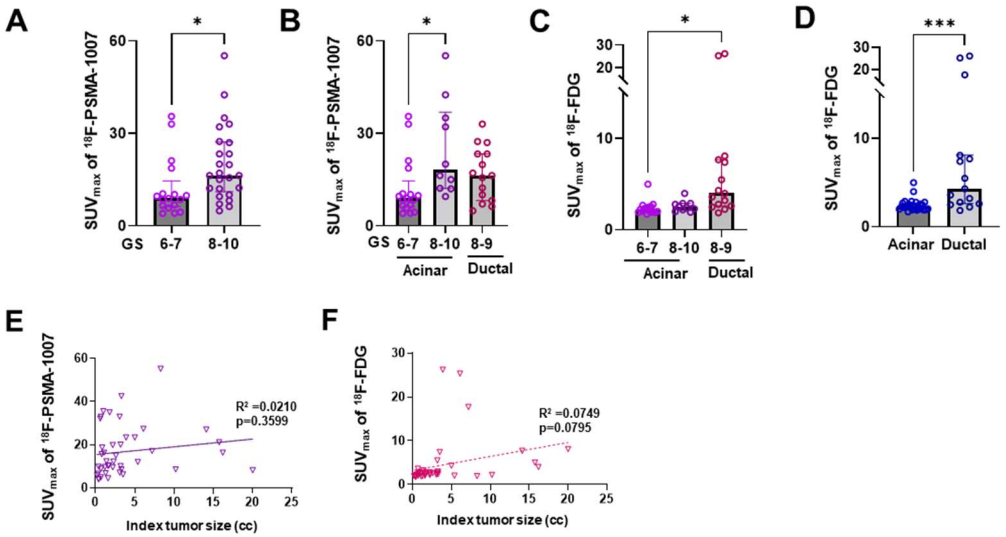

Figure 1. The SUV_{max} of ^{18}F-PSMA-1007 and ^{18}F-FDG in PCa patients. (A) The SUV_{max} of ^{18}F-PSMA-1007 according to GS in 42 index tumors. (B, C) The SUV_{max} of ^{18}F-PSMA 1007 (B) ^{18}F-FDG (C) according to GS and in acinar dominant tumor (n= 27), ductal dominant tumor (n= 15). (D) The SUV_{max} of ^{18}F-FDG according to histological subtype in 42 index tumors. (E-F) The correlation between the index tumor of ^{18}F-PSMA-1007 and ^{18}F-FDG. Index tumor size Data are presented as median and statically analyzed by unpaired two-tailed t-test. **P < 0.05, ***P < 0.001.

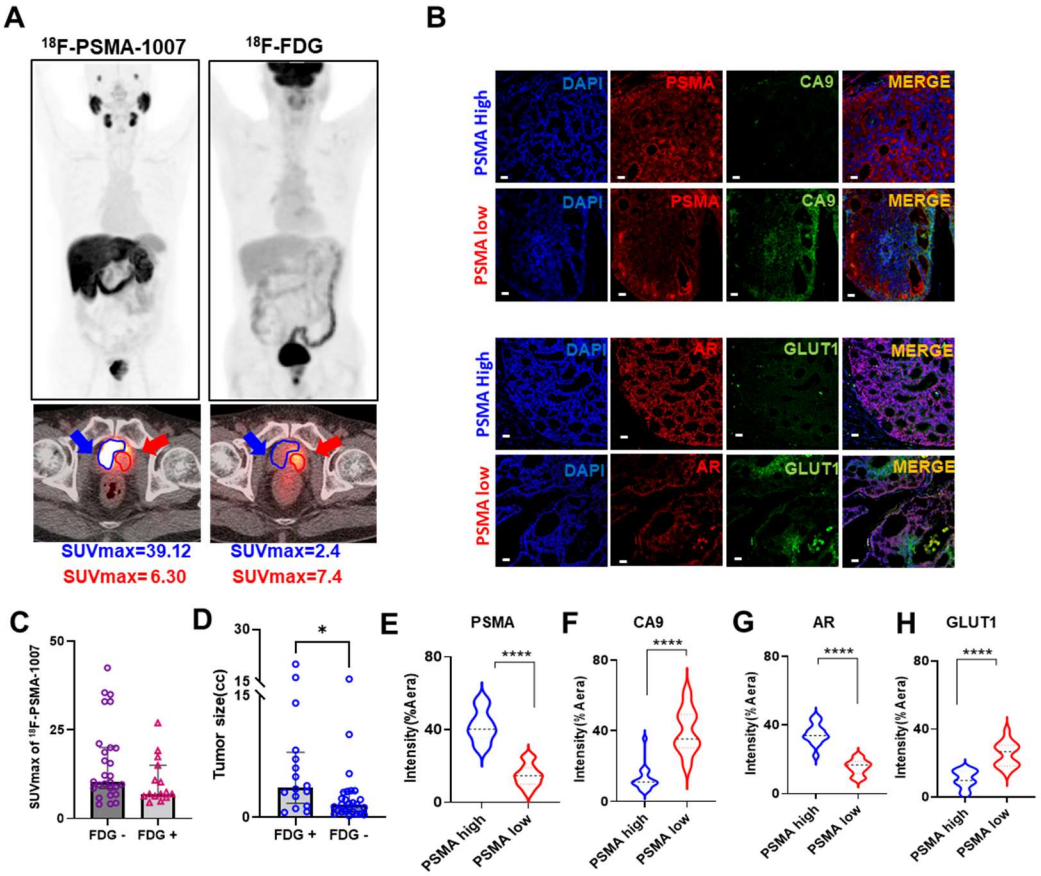

Figure 2. Representative ^{18}F-PSMA-1007 and ^{18}F-FDG PET/CT transaxial images in FDG positive patient and immunofluorescence. (A) Representative ^{18}F-PSMA-1007 and ^{18}F-FDG PET/CT whole body and axial images in ductal type. (B) Immunofluorescence of FDG positive PCa patients. (C) The SUV_{max} of ^{18}F-PSMA-1007 of FDG positive patients between FDG positive uptake region and PSMA positive uptake region. (D) The index tumor size between FDG positive patients and FDG negative patients. (E-H) The intensity of PSMA, CA9, AR and GLUT1 expression. Nuclei were counterstained with DAPI. Scale bars: 50 μm.*P < 0.05, ****P < 0.0001.

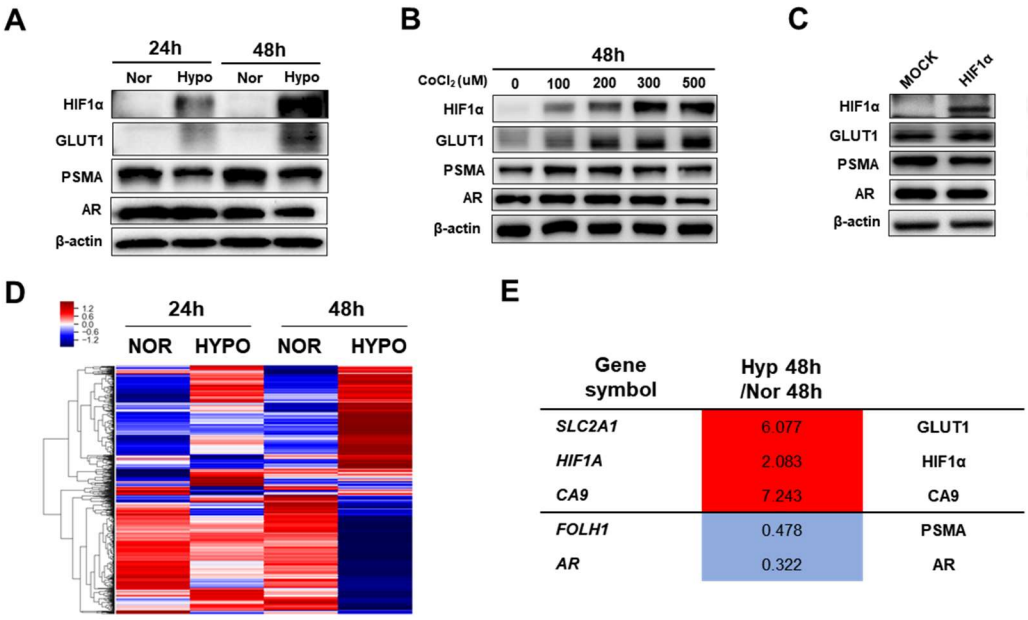

Figure 3. Downregulation of PSMA in glycolytic PCa cells in vitro. (A) HIF1α, GLUT1, PSMA, AR and β-actin expression levels in LNCaP cells under 21% or 1% O_2 for 24h and 48h. (B) (A) HIF1α, GLUT1, PSMA, AR and β-actin expression levels in LNCaP cells after treatment with indication concentration of $CoCl_2$ for 48h. (C) HIF1α, GLUT1, PSMA, AR and β-actin expression levels after transfection with MOCK or HIF1α plasmid for 48h. (D) Heat map representing color-coded expression levels of differentially expressed genes (p-value>0.05, normalized data(log2)>4, up- or down-regulated>1.5-fold) in LNCaP cells under 21% or 1% O_2 for 24 h and 48h. (E) Fold change of indicated genes in gene array analysis of (D).

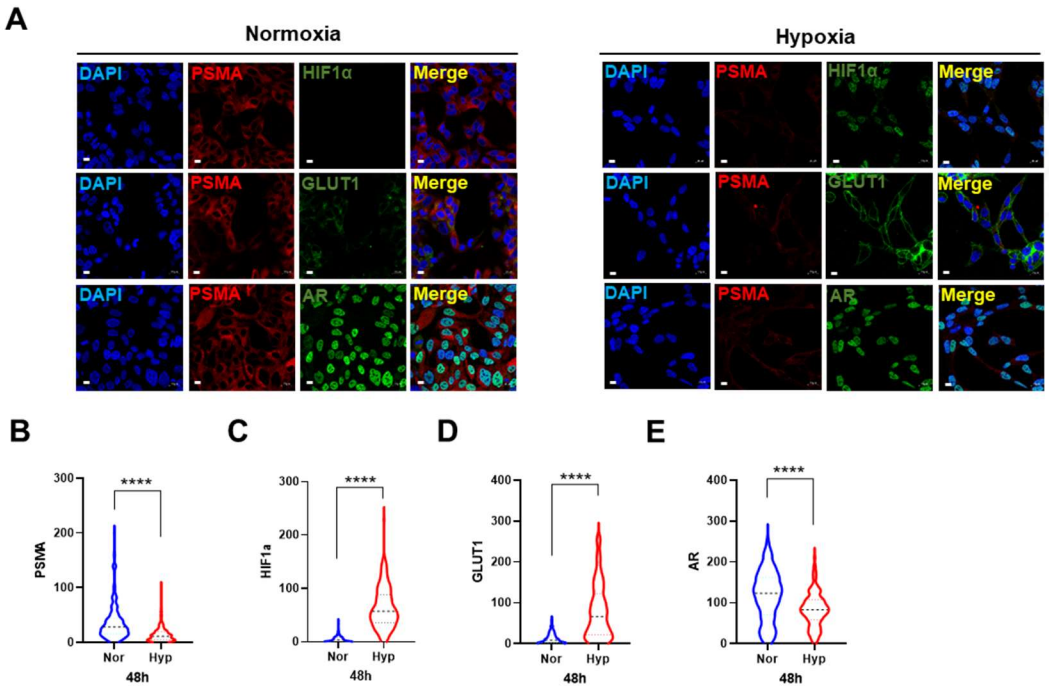

Figure 4. Immunocytochemistry of PSMA, HIF1α and GLUT1 using LNCaP cells under 21% (normoxia, left) or 1% O_2 (hypoxia, right) for 48h (A). Nuclei were counterstained with DAPI. Scale bars: 50 μm. (B-E) Quantification of positive reactivity in PSMA (B), HIF1α (C), GLUT1 (D) and AR (E) positive cells.

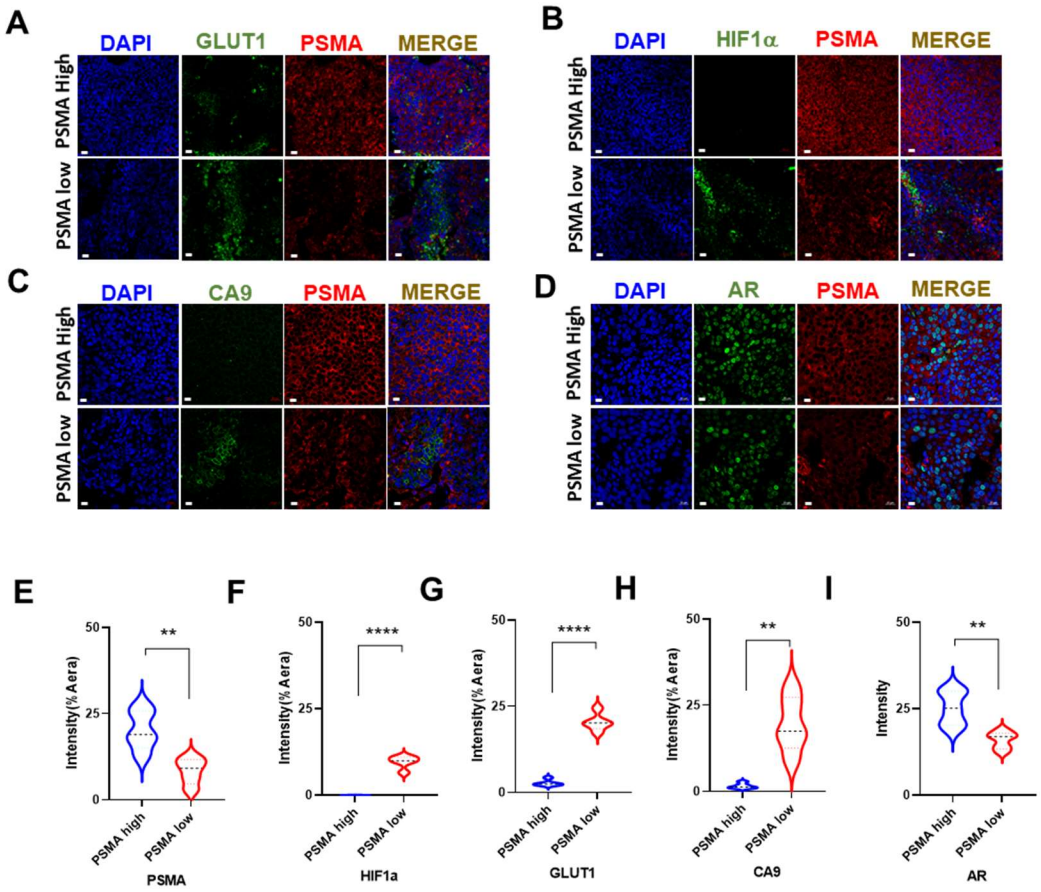

Figure 5. Downregulation of PSMA in glycolytic PCa in LNCaP-xenograft animal model. (A-D) Co-immunofluorescence of PSMA and GLUT1 (A), PSMA and HIF1α (B), PSMA and CA9 (C), and PSMA and AR. Nuclei were counterstained with DAPI. Scale bars: 20 μm. (E-I) Quantification of positive reactivity intensity of PSMA (E), HIF1α (F), GLUT1 (G), CA9 (H) and AR (I). Immunofluorescence was performed with indicated antibodies and nuclei were counterstained with DAPI. Scale bars: 20 μm.

IV. DISCUSSION

Various PET radiotracers of specific molecular targets have been used as a promising imaging modality for cancer diagnosis. Among them, ^{18}F-FDG is the most widely available PET trace used for staging cancers, predicting the tumor recurrences and therapeutic response. However, the clinical utility of ^{18}F-FDG PET/CT in detecting PCa has been conflicting in several studies. Recently, to detect the precise PCa staging, ^{18}F-PSMA PET/CT were developed and considered as an emerging imaging method in detecting PCa lesions. Here, we demonstrated that ^{18}F-PSMA PET/CT can be useful for the evaluation of GS in acinar types. In addition, there was a reciprocal pattern of PSMA and glycolysis-related proteins, suggesting that the possibility of the combination with ^{18}F-PSMA PET and of ^{18}F-FDG PET for detecting of PCa with high glycolysis under hypoxia.

The traditional diagnosis for PCa is digital rectal examination and PSA blood test. Despite serum PSA is a tissue-specific and sensitive tumor marker, the PSA level itself does not provide information regarding the origin of the PSA, such as benign prostatic hyperplasia (BPH), prostatitis, inflammation of the prostate that raise serum PSA levels [14]. Thus, the development of accurate imaging is required as an effective diagnostic tool to detect, localize, and characterize PCa. Currently, ^{11}C-Choline and ^{18}F-fluciclovine (Axumin™) have been clinically used for the identification of PCa. However, specificity of these PET tracers is limited to detection of primary PCa. For instance, ^{11}C-choline targeting choline transport also showed high uptake in benign prostatic hyperplasia. Recently, PSMA-targeted PET tracer has gained Food and Drug Administration (FDA) approval for PCa.^{68}Ga-PSMA showed more accuracy as compare with ^{11}C-Choline [15] and a significant difference in tracer uptake with a GS of 7-10 versus 6 or less [16]. Also, a large retrospective study by Oromieh et al., found a trend between higher GS and detection rates of ^{68}Ga-PSMA of patients with recurrent PCa (n=1007), albeit this was not statistically significant.

^{68}Ga-labeled compounds have the short half-life and relatively low available radioactivity, thus ^{18}F-labeled PSMA ligand have been developed. ^{18}F-PSMA-1007 was

able the high detection rates of recurrent tumor site within the prostate and surrounding pelvic structures after prostatectomy compared to ^{68}Ga-labeled PSMA ligand [17]. Also, Hong et al., reported that PCa with low grade (GS 6 and 7a) showed significantly lower ^{18}F-PSMA-1007 uptake compared to patients with high grade (GS 8 and 9). Our study also found the positive correlation between SUV_{max} of ^{18}F-PSMA-1007 and GS, but unlike other studies, we found the lower SUV_{max} of ^{18}F-PSMA-1007 in ductal type compared with acinar type with same GS.

Ductal type is a rare variant of PCa that is considered as more aggressive with a poor prognosis and limited therapeutic options than pure acinar type [18]. It has been known that PCa does not exhibit the Warburg effect, as these cells do not have the increased glucose uptake seen in many other cancers [19]. However, here we illustrated higher ^{18}F-FDG uptake and GLUT1 expression in PCa patients with high GS, mainly ductal dominant type, suggesting that PCa cells has ability to switch to a high glycolytic tumor cells. In line with our studies, the other studies demonstrated primary PCa with GS >7 tend to display high ^{18}F-FDG uptake [20]. Indeed, our study also indicated that there is no significant correlation of the SUV_{max} of ^{18}F-FDG and serum PSA in ductal type not acinar type. Moreover, serum PSA levels were found to be significantly lower in patients with ductal type, suggesting that only ^{18}F-FDG FDG could detect the aggressive ductal PCa [21].

A recent prospective study found negative ^{68}Ga-PSMA and positive of ^{18}F-FDG uptake in 29% of tumor lesion out of 114 lesions from 24 patients with PCa. Moreover, significant portion of PCa patients with metastatic disease showed negative ^{68}Ga-PSMA and positive of ^{18}F-FDG uptake, and an early PSA progression during castration [22]. Also, PCa patients including tumor lesions with negative PSMA and positive FDG uptake showed higher GS compared with PCa patients without these tumor lesions [23]. To the best of our knowledge, we demonstrated for the first-time hypoxic condition induced downregulation of PSMA, resulting in higher uptake of ^{18}F-FDG and lower uptake of ^{18}F-PSMA-1007. Moreover, the ^{18}F-FDG-positive tumor volume of PCa might be associated with poor survival in patients undergoing therapy targeting PSMA. Indeed, downregulation of PSMA expression in PCa

cell lines was increased tumor invasiveness *in vitro* [24]. In our study, the expression of AR was reduced in glycolytic PCa cells. Recent studies reported stronger inhibition of the AR signaling axis induced AR epigenetic silencing and protein loss, resulting in AR-negative de-differnetiated PCa with castration-resistant and poor prognosis [25]. Also, the increased expression of AR induced the repression of neuroendocrine tumors (NET) markers in LNCaP cells [26]. In our study, NET-related genes were dysregulated in LNCaP cells under hypoxic condition in our global gene array analysis, suggesting that glycolytic condition can be associated with induction of de-differnetated PCa [7, 27-29]. Thus, the reprogramming of glycolysis might be a good strategy for patients with castration-resistant prostate cancer (CRPC).

In conclusion, we confirmed ^{18}F-PSMA 1007 PET/CT was a useful imaging modality predicating staging of PCa of patients with acinar type. In addition, there is a contrasting pattern of ^{18}F-FDG uptake and ^{18}F-PSMA 1007 PET/CT in mainly ductal PCa with high GS. We also discovered reduced uptake pf ^{18}F-PSMA 1007 PET/CT might be due to increased glycolysis by hypoxic condition. Thus, the combination with ^{18}F-PSMA PET and of ^{18}F-FDG PET can be a potential strategy detecting for PCa with poor prognosis.

V. CONCLUSION

In our study, 42 index tumors of a total of 42 PCa patients were classified using the Gleason score and histological subtype. Using this, the SUV_{max} of ^{18}F-PSMA-1007 and ^{18}F-FDG of the index tumor were analyzed, and it was confirmed that the index tumor of the patient showing FDG positive was the ductal dominant type, and the PSMA uptake at that location was lowered. This fact was designed in consideration of the correlation with hypoxic condition in which glucose uptake increases, and it can be confirmed that PSMA decreased when a marker of hypoxia or glucose uptake was increased both *in-vivo* and *in-vitro*.

At the same time, it can be confirmed that AR is reduced, which shows that AR-targeted treatment is not suitable when early PET/CT shows FDG positive uptake. In the future, when diagnosing and treating prostate cancer patients at an early stage, if they show FDG positive, treatment should be carried out in a way other than AR target treatment.

REFERENCES

1. Rawla P: **Epidemiology of Prostate Cancer**. *World J Oncol* 2019, **10**(2):63-89.
2. Descotes JL: **Diagnosis of prostate cancer**. *Asian J Urol* 2019, **6**(2):129-136.
3. Troyer JK, Beckett ML, Wright GL, Jr.: **Detection and characterization of the prostate-specific membrane antigen (PSMA) in tissue extracts and body fluids**. *Int J Cancer* 1995, **62**(5):552-558.
4. Oh SW, Cheon GJ: **Prostate-Specific Membrane Antigen PET Imaging in Prostate Cancer: Opportunities and Challenges**. *Korean J Radiol* 2018, **19**(5):819-831.
5. Jang M, Kim SS, Lee J: **Cancer cell metabolism: implications for therapeutic targets**. *Exp Mol Med* 2013, **45**.
6. Almuhaideb A, Papathanasiou N, Bomanji J: **F-18-FDG PET/CT Imaging In Oncology**. *Ann Saudi Med* 2011, **31**(1):3-13.
7. Shen K, Liu B, Zhou X, Ji YY, Chen L, Wang Q, Xue W: **The Evolving Role of F-18-FDG PET/CT in Diagnosis and Prognosis Prediction in Progressive Prostate Cancer**. *Front Oncol* 2021, **11**.
8. Calais J, Czernin J: **PSMA Expression Assessed by PET Imaging Is a Required Biomarker for Selecting Patients for Any PSMA-Targeted Therapy**. *J Nucl Med* 2021, **62**(11):1489-1491.
9. Zhou X, Li YC, Jiang X, Wang XX, Chen SR, Shen TP, You JH, Lu H, Liao H, Li Z *et al*: **Intra-Individual Comparison of 18F-PSMA-1007 and 18F-FDG PET/CT in the Evaluation of Patients With Prostate Cancer**. *Front Oncol* 2021, **10**.
10. Shi YP, Xu L, Zhu YJ, Wang YN, Chen RH, Liu JJ: **Use of Ga-68-PSMA-11 and F-18-FDG PET-CT Dual-Tracer to Differentiate Between Lymph Node Metastases and Ganglia**. *Front Oncol* 2021, **11**.
11. Lee M, Jeon JY, Neugent ML, Kim JW, Yun M: **18F-Fluorodeoxyglucose uptake on positron emission tomography/computed tomography is associated with metastasis and epithelial-mesenchymal transition in hepatocellular carcinoma**. *Clin Exp Metastas* 2017, **34**(3-4):251-260.
12. Lee M, Marinoni I, Irmler M, Psaras T, Honegger JB, Beschorner R, Anastasov N, Beckers J, Theodoropoulou M, Roncaroli F *et al*: **Transcriptome analysis of MENX-associated rat pituitary adenomas identifies novel molecular mechanisms involved in the pathogenesis of human pituitary gonadotroph adenomas**. *Acta Neuropathol* 2013, **126**(1):137-150.
13. Jo H, Lee J, Jeon J, Kim SY, Chung JI, Ko HY, Lee M, Yun MJ: **The critical role of glucose deprivation in epithelial-mesenchymal transition in hepatocellular carcinoma under hypoxia**. *Sci Rep-Uk* 2020, **10**(1).
14. Cakir SS, Polat EC, Ozcan L, Besiroglu H, Otunctemur A, Ozbek E: **The effect of prostatic inflammation on clinical outcomes in patients with benign prostate hyperplasia**. *Prostate Int* 2018, **6**(2):71-74.
15. Hegemann NSS, Rogowski P, Eze C, Schafer C, Stief C, Lang S, Spohn S, Steffens R, Li ML, Gratzke C *et al*: **Outcome After 68Ga-PSMA-11 versus Choline PET-Based Salvage Radiotherapy in Patients with Biochemical Recurrence of Prostate Cancer: A Matched-Pair Analysis**. *Cancers* 2020, **12**(11).
16. Grubmuller B, Baltzer P, Hartenbach S, D'Andrea D, Helbich TH, Haug AR, Goldner GM, Wadsak W, Pfaff S, Mitterhauser M *et al*: **PSMA Ligand PET/MRI for Primary Prostate**

Cancer: Staging Performance and Clinical Impact. *Clin Cancer Res* 2018, **24**(24):6300-6307.

17. Giesel FL, Knorr K, Spohn F, Will L, Maurer T, Flechsig P, Neels O, Schiller K, Amaral H, Weber WA *et al*: **Detection Efficacy of F-18-PSMA-1007 PET/CT in 251 Patients with Biochemical Recurrence of Prostate Cancer After Radical Prostatectomy**. *J Nucl Med* 2019, **60**(3):362-368.
18. Montironi R, Cimadamore A, Lopez-Beltran A, Scarpelli M, Aurilio G, Santoni M, Massari F, Cheng L: **Morphologic, Molecular and Clinical Features of Aggressive Variant Prostate Cancer**. *Cells-Basel* 2020, **9**(5).
19. Liberti MV, Locasale JW: **The Warburg Effect: How Does it Benefit Cancer Cells? (vol 41, pg 211, 2016)**. *Trends Biochem Sci* 2016, **41**(3):287-287.
20. Sahin E, Elboga U, Kalender E, Basibuyuk M, Demir HD, Celen YZ: **Clinical significance of incidental FDG uptake in the prostate gland detected by PET/CT**. *Int J Clin Exp Med* 2015, **8**(7):10577-10585.
21. Morgan TM, Welty CJ, Vakar-Lopez F, Lin DW, Wright JL: **Ductal Adenocarcinoma of the Prostate: Increased Mortality Risk and Decreased Psa Secretion**. *J Urology* 2010, **183**(4):E95-E96.
22. Wang BH, Liu C, Wei Y, Meng J, Zhang YJ, Gan HL, Xu XP, Wan FN, Pan J, Ma XJ *et al*: **A Prospective Trial of Ga-68-PSMA and F-18-FDG PET/CT in Nonmetastatic Prostate Cancer Patients with an Early PSA Progression During Castration**. *Clin Cancer Res* 2020, **26**(17):4551-4558.
23. Chen RH, Wang YN, Zhu YJ, Shi YP, Xu L, Huang G, Liu JJ: **The Added Value of F-18-FDG PET/CT Compared with Ga-68-PSMA PET/CT in Patients with Castration-Resistant Prostate Cancer**. *J Nucl Med* 2022, **63**(1):69-75.
24. Ghosh A, Wang YN, Klein E, Heston WDW: **Novel role of prostate-specific membrane antigen in suppressing prostate cancer invasiveness**. *Cancer Res* 2005, **65**(3):727-731.
25. Formaggio N, Rubin MA, Theurillat JP: **Loss and revival of androgen receptor signaling in advanced prostate cancer**. *Oncogene* 2021, **40**(7):1205-1216.
26. Zhang Y, Zheng DY, Zhou T, Song HP, Hulsurkar M, Su N, Liu Y, Wang Z, Shao L, Ittmann M *et al*: **Androgen deprivation promotes neuroendocrine differentiation and angiogenesis through CREB-EZH2-TSP1 pathway in prostate cancers**. *Nat Commun* 2018, **9**.
27. Bhagirath D, Liston M, Akoto T, Lui B, Bensing BA, Sharma A, Saini S: **Novel, non-invasive markers for detecting therapy induced neuroendocrine differentiation in castration-resistant prostate cancer patients**. *Sci Rep-Uk* 2021, **11**(1).
28. Kim S, Thaper D, Bidnur S, Toren P, Akamatsus S, Bishop JL, Colins C, Vahid S, Zoubeidi A: **PEG10 is associated with treatment-induced neuroendocrine prostate cancer**. *J Mol Endocrinol* 2019, **63**(1):39-49.
29. Kivinummi K, Urbanucci A, Leinonen K, Tammela TLJ, Annala M, Isaacs WB, Bova GS, Nykter M, Visakorpi T: **The expression of AURKA is androgen regulated in castration-resistant prostate cancer**. *Sci Rep-Uk* 2017, **7**.

APPENDICES

1. Abbreviation

PSMA : Prostate-specific membrane antigen

PET/CT : Positron emission tomography / Computed tomography

^{18}F-FDG : [^{18}F]Fluorodeoxyglucose

SUV_{max} : Standardized uptake value max

AR : Androgen receptor

CA9 : Carbonic anhydrase 9

HIF1a : Hypoxia-inducible factor 1 alpha

GLUT1 : Glucose uptake transporter 1

IF : Immunofluorescence

ICC : Immunocytochemistry

IHC : Immunohistochemistry

ABSTRACT(IN KOREAN)

전립선암에서 암 대사에 따른 ^{18}F-PSMA-1007 와 ^{18}F-FDG의 PET/CT 영상 분석

<지도교수 윤미진>

연세대학교 대학원 의학과

김지수

전립선암은 전립선의 악성 종양으로 전 세계적으로 암으로 사망하는 남성 중 두 번째로 흔한 암으로 알려져 있다. 전립선 특이적 항원 (PSA) 혈액 검사는 일반적으로 초기 단계에 수행되며 혈액 내 전립선 특이적 항원 수치가 높을수록 전립선암일 가능성이 높다. 그러나 전립선 특이적 항원 수치가 높은 남성의 약 25%만이 실제로 생검을 통해 전립선암 진단을 받는다. 따라서 전립선암 진단의 초기 단계에서 보다 안정적이고 정확한 전립선암 진단 및 검출 방법이 필요하다.

전립선 특이적 막 항원(PSMA)은 전립선암에 특이적인 효소이며 인간 *FOLH1* 유전자에 의해 암호화된다. 전립선암 환자에서 정상 전립선에 비해 전립선 특이적 막 항원 의 발현이 증가함을 확인하였다. 전립선암에서 전립선 특이적 막 항원 의 발현 정도는 전립선암의 병리학적 상태에 따라 달라지는데 이는 환자의 예후와 밀접한 관련이 있다. 이러한 전립선 특이적 막 항원 의 발현 정도의 차이는 전립선암 환자에게 유용한 영상 표적이 될 수 있으며,

양전자 단층 촬영(PET/CT)을 통한 전립선암의 진단 및 치료에 활용되고 있다.

암세포는 비정상적인 혈관 형성과 성장으로 저산소증을 유발한다. 저산소증으로 유발된 암에서 여러 단백질의 발현은 저산소증 유발 인자 (HIF)에 의해 유도되거나 억제될 수 있다. 또한 와버그 효과(Warburg effect)로 인해 포도당 대사가 증가하고 포도당 흡수율이 증가하여 포도당 수송 경로 단백질 (GLUTs) 의 발현이 증가하여 포도당 표적 양전자 단층 촬영 영상 추적이 가능하다.

따라서 전립선암에서도 전립선 특이적 막 항원과 함께 ^{18}F-FDG 흡수를 이용한 영상 분석을 통해 암의 악성도를 추적할 수 있다. ^{18}F-PSMA-1007 과 ^{18}F-FDG 양전자 단층 촬영 영상 간의 SUV_{max} 를 비교하고 *in-vivo* 와 *in-vitro* 에서 전립선 특이적 막 항원 발현을 분석하여 초기 전립선암에 대한 새로운 진단 기준을 찾으려 한다.

핵심되는 말 : 전립선 특이적 막 항원, 포도당 수송 단백질 1, 양전자 단층 촬영, ^{18}F-PSMA-1007, ^{18}F-FDG, 저산소증